EURODYN 2020
XI International Conference on Structural Dynamics
M. Papadrakakis, M. Fragiadakis, C. Papadimitriou (eds.)
Athens, Greece, 23—25 November 2020

AN IN-SITU EXPERIMENTAL SETUP FOR DAMAGE LOCALIZATION AND MECHANICAL PARAMETER ESTIMATION

M. Vollmering[1], I. Dolbonosov[1], A. Lenzen[1]

[1]Institute for Statics, Structural Dynamics, System Identification, and Simulation (I4S)
Leipzig University of Applied Sciences, Karl-Liebknecht-Straße 132, 04277 Leipzig
e-mail: Armin.Lenzen@htwk-leipzig.de

Keywords: Output-only identification, Damage localization, H-infinity estimation, Mechanical parameter estimation, Mass perturbation methods, Projection techniques in state space

Abstract. *A new in-situ experimental setup for damage localization and mechanical parameter estimation has been built at two test fields, outdoors at a rooftop and in a laboratory at Leipzig University of Applied Sciences. Excited by wind, the structure can be identified by output-only methods. In this contribution current progress on the development of damage localization and scaling output-only systems from a general operator notation is shown. At the beginning damage localization based on $\mathcal{H}_\infty$-estimation is briefly shown. Modifying this theory, system scaling and mechanical parameter estimation is discussed afterwards. Finally, experimental results are shown and analysed.*

1 Introduction

In structural dynamics the parametrization of a mechanical model allows to analyse system properties and predict structural responses in certain load cases. To parametrize real life structures, a *linear-elastic* mechanical model is often a well-suited approximation at an operation point, which is modelled by mass, stiffness, and damping ($\bar{M}$, $\bar{K}$, and $\bar{D}$). To avoid a priori model errors and a possible huge numerical effort, *system identification* allows a straightforward alternative parametrization of a mechanical model, which the authors focus in this contribution. Directly based on measurements, the identified system has a considerably smaller model order. Here, the parametrization of a *linear, time-invariant state space system* is very advantageous, as this allows to subsequently apply identified parameters in other techniques.

Stochastic system identification. Because deterministic excitations are cost-intensive, elaborate, and sometimes impossible to apply at large-scale civil engineering structures, identification methods based on *ambient excitations* (e.g. wind, traffic, waves, microseism) should be applied instead [1]. Some stochastic system identification methods are a) stochastic realization [2], b) stochastic subspace identification (SSI) [3], c) canonical correlation analysis (CCA) [4], and so on. Because ambient excitations are in general unmeasurable, state space parameters A and C can be determined only based on structural response measurements. Hence, the physical interpretation of the identified system is an important issue. A widespread approach is the identification of modal data (free scaled mode shapes), named operational modal analysis (OMA) [5–7]. However, without the necessity of numerical computations based on (real or complex-conjugated) mode shapes, we focus on the development of a general, system theoretic identification approach.

Motivation: Mechanical parameter estimation and damage localization. A new in-situ experimental setup for damage localization and mechanical parameter estimation has been built at two test fields, outdoors at a rooftop and in a laboratory at Leipzig University of Applied Sciences (see figure 1 and section 4). Excited by wind, the structure can be identified by output-

(a) Wind-exposed structure at a rooftop (b) Laboratory structure

Figure 1: Experimental structures

only methods. The authors aim to develop and verify a damage localization method based on the *state projection estimation error* (SP2E) [8–11], which is insensitive to environmental and operational conditions (EOC). While first attempts based on principal component analysis were analysed [12], a system theoretic approach may be advantageous.

In this contribution, current progress on the development of damage localization and scaling output-only systems from a general operator notation is shown. To begin with in section 2, damage localization based on SP2E is briefly shown. Modifying this theory, the novel *state projections for system scaling* (SP2S) method and subsequent mechanical parameter estimation is discussed afterwards, which is based on output-only measurements and the mass perturbation technique (repetition of measurement with known additional mass Δ_M, section 3). Finally, experimental results are shown and analysed in section 4.

Some notes on the used nomenclature. Because structural alterations are a key element of this contribution (e.g. stiffness modifications $\Delta_{K,i}$ and/or *mass perturbations* $\Delta_{M,i}$), the definition of structural state i is introduced: $i = 0$ defines the reference and $i > 0$ the altered structural state.

We focus on the application of estimation/control approaches in structural dynamics. Hence, a more general system theoretic notation is used: The map to y from u is denoted by T_{yu}. By using a linear, time-invariant state space system, T_{yu} may be written in frequency domain as

$$\left.\begin{aligned} \sigma x(\sigma) &= Ax(\sigma) + Bu(\sigma) \\ y(\sigma) &= Cx(\sigma) + Du(\sigma) \end{aligned}\right\} \sigma = (s, z) \; .$$

Based on state space parameters A, B, C, and D, the frequency response matrix function follows:

$$T_{yu}(\sigma) = \left[\begin{array}{c|c} A & B \\ \hline C & D \end{array}\right] \overset{\sigma}{=} C\big(\sigma I - A\big)^{-1}B + D \; .$$

2 Damage localization based on $\mathcal{H}_\infty$-estimation: State projection estimation error (SP2E)

2.1 Basis: Output-only identification

As mechanical system parameters ($\bar{M}$, $\bar{K}$, and $\bar{D}$) and structural excitations are unknown for real large-scale structures, we use the SSI [3] to parametrize discrete-time state space parameters A and C. These matrices are applied to define a *discrete-time system*

$$\begin{bmatrix} x_{k+1} \\ y_k \end{bmatrix} = \left[\begin{array}{c|cc} A & I & 0 \\ \hline C & 0 & I \end{array}\right] \begin{bmatrix} x_k \\ w_k \\ v_k \end{bmatrix} , \quad n_k = \begin{bmatrix} w_k \\ v_k \end{bmatrix} \quad \text{with } \big\langle n_k, n_k \big\rangle := \begin{bmatrix} Q & S \\ S^* & R_v \end{bmatrix} . \tag{1}$$

2.2 $\mathcal{H}_\infty$-estimation: Worst-case analysis

$\mathcal{H}_\infty$-theory leads to estimators, which are less susceptible to *disturbance uncertainties*. A key element for that is to consider the so-called worst-case. Hence, one uses the $\mathcal{H}_\infty$-norm to bound a system $T_{\tilde{s}n}$ by γ, which is equivalent to bound the largest singular value of matrix function $T_{\tilde{s}n}$, namely

$$\|T_{\tilde{s}n}\|_{\mathcal{H}_\infty} = \sup_n \frac{\|\tilde{s}\|_2}{\|n\|_2} = \max_\omega \bar{\sigma}\Big(T_{\tilde{s}n}(e^{j\omega})\Big) < \gamma \; , \quad \tilde{s} = s - \hat{s} = L\big(x - \hat{x}\big) = L\tilde{x} \; . \tag{2}$$

Although $\mathcal{H}_\infty$-theory may lead to over-conservative estimators, they outperform Kalman filters ($\mathcal{H}^2$ estimators), when the disturbances are unknown [13]. An important difference to Kalman filtering is the usage of weighting parameter L, allowing different applications in $\mathcal{H}_\infty$-estimation [13]. For the case of *filtering signals in additive noise* [14] one uses $L = C$.

There are plenty $\mathcal{H}_\infty$-theory approaches [13–17]. A powerful, theoretical approach is the derivation of estimation as *a special case of control* by using the lower linear fractional transformation (LLFT, see figure 2) [18]:

$$\begin{bmatrix} x_{k+1} \\ \tilde{s}_k \\ y_k \end{bmatrix} = \underbrace{\left[\begin{array}{c|cc} A & \begin{bmatrix} I & 0 \end{bmatrix} & 0 \\ \hline L & \begin{bmatrix} 0 & 0 \end{bmatrix} & -I \\ C & \begin{bmatrix} 0 & I \end{bmatrix} & 0 \end{array}\right]}_{P} \begin{bmatrix} x_k \\ w_k \\ v_k \\ \hat{s}_k \end{bmatrix}, \qquad \begin{bmatrix} \hat{x}_{k+1} \\ \hat{s}_k \end{bmatrix} \underbrace{\left[\begin{array}{c|c} A - K_p C & K_p \\ \hline L & 0 \end{array}\right]}_{K} \begin{bmatrix} \hat{x}_k \\ y_k \end{bmatrix} . \tag{3}$$

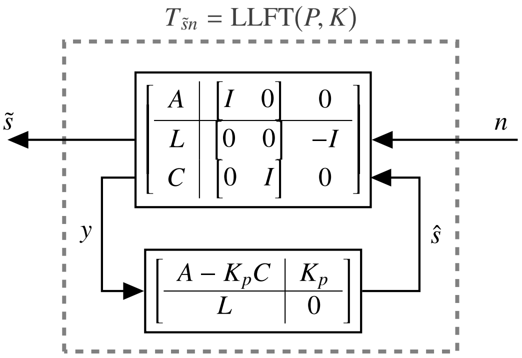

Figure 2: Estimation as a special case of control

LMI based $\mathcal{H}_\infty$-estimation. Linear matrix inequality (LMI) methods are widespread to determine $\mathcal{H}_\infty$-controllers [19, 20]. Based on the bounded real lemma, a γ-optimal controller K exists in discrete-time (see equation (2)) in both equivalent expressions

$$\left\| T_{\tilde{s}n}\big(\mathcal{A}_{cl}, \mathcal{B}_{cl}, \mathcal{C}_{cl}, \mathcal{D}_{cl}\big) \right\|_{\mathcal{H}_\infty} < \gamma, \quad \mathcal{H} = \begin{bmatrix} -\mathcal{X}^{-1} & \mathcal{A}_{cl} & \mathcal{B}_{cl} & 0 \\ \mathcal{A}_{cl}^T & -\mathcal{X} & 0 & \mathcal{C}_{cl}^T \\ \mathcal{B}_{cl}^T & 0 & -\gamma^2 I & \mathcal{D}_{cl}^T \\ 0 & \mathcal{C}_{cl} & \mathcal{D}_{cl} & -I \end{bmatrix} < 0 \,, \tag{4}$$

if the above inequality is feasible for $\mathcal{X} > 0$. Hence, an *optimization problem* follows, namely the minimization of γ under the above constraints, which may be solved numerically (see [21, 22]). A numerical minimum for γ^2 can be found by *semidefinite programming* (SDP), which may lead to the strictly proper form

$$\begin{bmatrix} \hat{x}_{k+1} \\ \hat{y}_k \end{bmatrix} = \underbrace{\left[\begin{array}{c|c} A_f & K_f \\ \hline C & 0 \end{array}\right]}_{K_{\mathrm{LMI}}} \begin{bmatrix} \hat{x}_k \\ y_k \end{bmatrix} . \tag{5}$$

Riccati recursion/equation based $\mathcal{H}_\infty$-estimation. Besides the LMI solution, the application of indefinite metric spaces for $\mathcal{H}_\infty$-estimation [14] is a remarkable theory. Based on the *minimization of an indefinite quadratic form* [23], this theory leads to a Riccati recursion

$$P_{k+1} = AP_k\left(I - \begin{bmatrix} L \\ C \end{bmatrix}^* \left(\begin{bmatrix} L \\ C \end{bmatrix} P_k \begin{bmatrix} L \\ C \end{bmatrix}^* + \begin{bmatrix} -\gamma^2 I & 0 \\ 0 & I \end{bmatrix} \right)^{-1} \begin{bmatrix} L \\ C \end{bmatrix} P_k \right) A^* + Q \tag{6a}$$

$$= A\left(P_k^{-1} - \gamma^{-2} L^* L + C^* C\right)^{-1} A^* + Q \; . \tag{6b}$$

To determine an $\mathcal{H}_\infty$-estimator, a convergent solution $P = P_{k+1} = P_k$ must be computed and important existence conditions are taken into account

$$\forall k: \quad \tilde{P}_k^{-1} = P_k^{-1} - \gamma^{-2} L^* L > 0, \quad P_k^{-1} - \gamma^{-2} L^* L + C^* C > 0 \; . \tag{7}$$

Because a direct recursive computation is numerically imprecise [24], one can solve a *discrete-time algebraic Riccati equation* (DARE) instead. To get a solution, the eigenvectors of an extended symplectic pencil are used to numerically determine matrix P [25], which leads to the *a priori* $\mathcal{H}_\infty$-estimator

$$\begin{bmatrix} \hat{x}_{k+1} \\ \hat{y}_k \end{bmatrix} = \underbrace{\left[\begin{array}{c|c} A_p & K_p \\ \hline C & 0 \end{array}\right]}_{K_{\text{DARE}}} \begin{bmatrix} \hat{x}_k \\ y_k \end{bmatrix} \quad \text{with } K_p = A\tilde{P}C^*\left(C\tilde{P}C^* + I\right)^{-1}, \quad A_p = A - K_p C \; . \tag{8}$$

As $\gamma \to \infty$, the estimator in equation (8) becomes the well-known Kalman filter (an $\mathcal{H}_2$-optimal estimator) [13].

2.3 Damage localization by state projection estimation error (SP2E) method

A difference process has been proposed for damage localization by the authors [9–11]. Process d follows the introduced system in discrete-time

$$\begin{bmatrix} \hat{x}_{0,k+1} \\ \hat{x}_{i,k+1} \\ x_{i,k+1} \\ d_k \end{bmatrix} = \underbrace{\left[\begin{array}{ccc|cc} A_{p,0} & 0 & K_{p,0}C_i & 0 & K_{p,0} \\ 0 & A_{p,i} & K_{p,i}C_i & 0 & K_{p,i} \\ 0 & 0 & A_i & I & 0 \\ \hline -C_0 & C_i & 0 & 0 & 0 \end{array}\right]}_{T_{dn}} \begin{bmatrix} \hat{x}_{0,k} \\ \hat{x}_{i,k} \\ x_{i,k} \\ w_k \\ v_k \end{bmatrix} . \tag{9}$$

Using state projections, a Sylvester equation must be solved, which leads to the following:

$$\begin{bmatrix} A_{p,0} & 0 \\ 0 & A_{p,i} \end{bmatrix} \bar{\Theta} - \bar{\Theta} A_i = - \begin{bmatrix} K_{p,0} \\ K_{p,i} \end{bmatrix} C_i \; , \quad \bar{\Theta} = \begin{bmatrix} Y \\ Z \end{bmatrix} \tag{10a}$$

$$\begin{bmatrix} \hat{x}_{0,k+1} \\ \hat{x}_{i,k+1} \\ x_{i,k+1} \\ d_{V,k} \end{bmatrix} = \underbrace{\left[\begin{array}{ccc|cc} A_{p,0} & 0 & 0 & -Y & K_{p,0} \\ 0 & A_{p,i} & 0 & -Z & K_{p,i} \\ 0 & 0 & A_i & I & 0 \\ \hline -C_0 & C_i & C_i Z - C_0 Y & 0 & 0 \end{array}\right]}_{T_{dVn}} \begin{bmatrix} \hat{x}_{0,k} \\ \hat{x}_{i,k} \\ x_{i,k} \\ w_k \\ v_k \end{bmatrix} . \tag{10b}$$

The SP2E difference process approach is a form of *model reduction*, namely the truncation of estimator poles. This has been discussed by the authors [9–11] and allows to define

$$\begin{bmatrix} x_{k+1} \\ d_{V,k} \end{bmatrix} = \underbrace{\left[\begin{array}{c|cc} A_i & I & 0 \\ \hline C_T & 0 & 0 \end{array}\right]}_{T_{dVn}} \begin{bmatrix} x_k \\ w_k \\ v_k \end{bmatrix} , \quad C_T = \begin{bmatrix} -C_0 & C_i \end{bmatrix} \begin{bmatrix} Y \\ Z \end{bmatrix} = C_i Z - C_0 Y \; . \tag{11}$$

As a result one determines the difference process d_V taking state projections into account. The average process power of d_V can be analysed for damage localization:

$$\bar{P}_{dV} = \mathrm{diag}\big(R_{dV}\big) \quad \text{with} \quad R_{dV} = \big\langle d_{V,k}, d_{V,k} \big\rangle \ . \tag{12}$$

The SP2E method has been verified based on experimental data and the study of damage localization results can be found in [9–11].

3 System scaling and mechanical parameter estimation based on output-only identification and mass perturbations

3.1 Relation of structural states in general operator notation

In this section some brief notes on the novel *state projections for system scaling* (SP2S) method and mechanical parameter estimation are given (for details see [26]). To find a relation for that, the constitutive equation of motion in structural dynamics is reordered to

$$a_i \stackrel{s}{=} T_{af,i} f : \qquad \bar{M} a_i(t) + \bar{D} v_i(t) + \bar{K} d_i(t) = f(t) - \Delta_{M,i} a_i(t) \ . \tag{13}$$

The mechanical system in reference structural state $T_{af,0}$ has the response of state i due to input $f - \Delta_{M,i} a_i(t)$ after a settling time (steady state vibrations). Omitting initial values, this may be expressed in Laplace domain by

$$a_i(s) = T_{af,0}(s)\Big(f(s) - \Delta_{M,i} a_i(s)\Big), \qquad T_{af,i} \stackrel{s}{=} T_{af,0}\big(I_p - \Delta_{M,i} T_{af,i}\big) \ . \tag{14}$$

In equation (14) we presuppose the same average excitation spectrum (in a stochastic sense) for both structural states $T_{af,0}$ and $T_{af,i}$. Equation (14) is very important to relate *reference and altered structural states in one framework* and a system description for the structural states is necessary to apply the found relation, which is shown below.

3.2 State projections for system scaling method (SP2S)

A state space approach is focused below, because this allows to apply standard system analysis techniques afterwards. Hence, by applying state space parameters A_i, B_i, C_i, and D_i in equation (14), one concludes the following in continuous-time:

$$\left[\begin{array}{c|c} A_i & B_i \\ \hline C_i & D_i \end{array}\right] \stackrel{s}{=} \left[\begin{array}{c|c} A_0 & B_0 \\ \hline C_0 & D_0 \end{array}\right] \left[\begin{array}{c|c} A_i & B_i \\ \hline -\Delta_{M,i} C_i & I_p - \Delta_{M,i} D_i \end{array}\right] \tag{15a}$$

$$\stackrel{s}{=} \left[\begin{array}{cc|c} A_0 & -B_0 \Delta_{M,i} C_i & B_0(I_p - \Delta_{M,i} D_i) \\ 0 & A_i & B_i \\ \hline C_0 & -D_0 \Delta_{M,i} C_i & D_0(I_p - \Delta_{M,i} D_i) \end{array}\right] \tag{15b}$$

$$a_i \stackrel{s}{=} T_{af,i} f : \qquad \begin{bmatrix} \dot{x}_0 \\ \dot{x}_i \\ a_i \end{bmatrix} = \left[\begin{array}{cc|c} A_0 & -B_0 \Delta_{M,i} C_i & B_0(I_p - \Delta_{M,i} D_i) \\ 0 & A_i & B_i \\ \hline C_0 & -D_0 \Delta_{M,i} C_i & D_0(I_p - \Delta_{M,i} D_i) \end{array}\right] \begin{bmatrix} x_0 \\ x_i \\ f \end{bmatrix} \ . \tag{15c}$$

In equation (15b) the state space system on the right-hand side has a considerably larger model order than the left-hand side. Applying the state projection technique of equation (10), a block diagonal form is determined:

$$A_0 \Theta_i - \Theta_i A_i = B_0 \Delta_{M,i} C_i \tag{16a}$$

$$\left[\begin{array}{c|c} A_i & B_i \\ \hline C_i & D_i \end{array}\right] \stackrel{s}{=} \left[\begin{array}{cc|c} A_0 & 0 & B_0(I_p - \Delta_{M,i} D_i) - \Theta_i B_i \\ 0 & A_i & B_i \\ \hline C_0 & C_0 \Theta_i - D_0 \Delta_{M,i} C_i & D_0(I_p - \Delta_{M,i} D_i) \end{array}\right] \ . \tag{16b}$$

Therefore, constraints are introduced to find a solution in accordance to state projection results:

$$-B_0\Delta_{M,i}C_i = \Theta_i A_i - A_0\Theta_i \tag{17a}$$
$$C_i = C_0\Theta_i - D_0\Delta_{M,i}C_i \tag{17b}$$
$$0 = B_0(I_p - \Delta_{M,i}D_i) - \Theta_i B_i \tag{17c}$$
$$D_i = D_0(I_p - \Delta_{M,i}D_i)\ . \tag{17d}$$

Using above, this leads to a solution to the model order problem of equation (15). A numerical efficient algorithm to solve the described problem is unknown to the authors so far. Hence, a rather theoretical approach based on the Kronecker product $\otimes$ is applied instead:

$$\mathcal{A}\mathcal{X}\mathcal{B} = \mathcal{C} \quad \longrightarrow \quad \Big(\mathcal{B}^T \otimes \mathcal{A}\Big)\mathrm{vec}\big(\mathcal{X}\big) = \mathrm{vec}\big(\mathcal{C}\big)\ . \tag{18}$$

The first two constraints of equation (17) are applied above, while the third and fourth are not used in the following. Using the Kronecker product approach, the set of constraints is reordered:

1. Constraint $-B_0\Delta_{M,i}C_i + A_0\Theta_i - \Theta_i A_i = 0$:

$$-\Big(C_i^T\Delta_{M,i}^T \otimes I_{n_0}\Big)\mathrm{vec}\big(B_0\big) + \Big((I_{n_i}\otimes A_0) - (A_i^T \otimes I_{n_0})\Big)\mathrm{vec}\big(\Theta_i\big) = 0\ . \tag{19}$$

2. Constraint $-D_0\Delta_{M,i}C_i + C_0\Theta_i = C_i$:

$$-\Big(C_i^T\Delta_{M,i}^T \otimes I_p\Big)\mathrm{vec}\big(D_0\big) + \Big(I_{n_i}\otimes C_0\Big)\mathrm{vec}\big(\Theta_i\big) = \mathrm{vec}\big(C_i\big)\ . \tag{20}$$

Because equations (19) and (20) are defined for i, both constraints can be used multiple times. Using A_i, C_i, and $\Delta_{M,i}$ ($i = 0,\ 1,\ \ldots$), both constraints are stacked together in a *system of linear equations*

$$\begin{bmatrix}\mathrm{vec}\big(B_0\big)\\ \mathrm{vec}\big(D_0\big)\\ \mathrm{vec}\big(\Theta_1\big)\\ \mathrm{vec}\big(\Theta_2\big)\\ \vdots\end{bmatrix} = \begin{bmatrix} -C_1^T\Delta_{M,1}^T\otimes I_{n_0} & 0 & (I_{n_1}\otimes A_0)-(A_1^T\otimes I_{n_0}) & 0 & \cdots\\ -C_2^T\Delta_{M,2}^T\otimes I_{n_0} & 0 & 0 & (I_{n_2}\otimes A_0)-(A_2^T\otimes I_{n_0}) & \\ \vdots & \vdots & \vdots & \vdots & \ddots\\ 0 & -C_1^T\Delta_{M,1}^T\otimes I_p & I_{n_1}\otimes C_0 & 0 & \cdots\\ 0 & -C_2^T\Delta_{M,2}^T\otimes I_p & 0 & I_{n_2}\otimes C_0 & \\ \vdots & \vdots & \vdots & \vdots & \ddots \end{bmatrix}^{\dagger} \begin{bmatrix}0\\ 0\\ \vdots\\ \mathrm{vec}\big(C_1\big)\\ \mathrm{vec}\big(C_2\big)\\ \vdots\end{bmatrix}\ . \tag{21}$$

This system of linear equations can be solved to estimate B and D of the structural reference state (e.g. by Tikhonov regularization). The described method is called *state projections for system scaling* (SP2S) and details can be found in [26].

3.3 Mechanical parameter estimation based on identified state space parameters

Using a Markov parameter approach, one may estimate mechanical properties based on continuous-time state space parameters A, B, and C [27]:

$$\hat{M} = \Big(C_0A_0^{1-m}B_0\Big)^{-1}\ ,\quad \hat{K} = -\Big(C_0A_0^{-1-m}B_0\Big)^{-1}\ ,\quad \hat{D} = -\hat{M}\Big(C_0A_0^{2-m}B_0\Big)\hat{M}\ . \tag{22}$$

Parameter m refers to the measurement type: Displacements $m = 0$, velocities $m = 1$, and accelerations $m = 2$.

3.4 Comparison to the mode shape based approach

Two important eigenvalue problems arise from the equation of motion in structural dynamics [28], which are briefly discussed below. To understand the real mode shape based mechanical parameter estimation problem, the eigenvalue problem

$$\big(- \bar{M}_i \omega_{i,l}^2 + \bar{K} \big) \phi_{i,l} = 0 \tag{23}$$

is shown first, which leads to real mode shapes $\Phi_i = [\phi_{i,1} \quad \phi_{i,2} \quad \ldots]$, $\Phi_i \in \mathbb{R}^{N_{dof} \times N_{dof}}$. A scaling factor α can be used to compute mass-normalized mode shapes $\bar{\phi}_l = \phi_l \alpha_l$. Based on identified real eigenvectors (e.g. by frequency domain decomposition), one needs scaled mode shapes to estimate mechanical parameters by

$$\hat{M}_i = \left[\sum_{l=1}^{n} \bar{\phi}_{i,l} \bar{\phi}_{i,l}^T \right]^{-1} , \quad \hat{K} = \left[\sum_{l=1}^{n} \frac{\bar{\phi}_{i,l} \bar{\phi}_{i,l}^T}{\omega_{i,l}^2} \right]^{-1} , \quad \hat{D} = \left[\sum_{l=1}^{n} \frac{\bar{\phi}_{i,l} \bar{\phi}_{i,l}^T}{2 \zeta_{i,l} \omega_{i,l}} \right]^{-1} . \tag{24}$$

Because real structures always have damping $\bar{D} > 0$, the eigenvalue problem in equation (23) may be generalized to

$$\begin{bmatrix} \bar{D} & \bar{M}_i \\ \bar{M}_i & 0 \end{bmatrix} \begin{bmatrix} \psi_{i,l} \\ \psi_{i,l} \lambda_{i,l} \end{bmatrix} \lambda_{i,l} + \begin{bmatrix} \bar{K} & 0 \\ 0 & -\bar{M}_i \end{bmatrix} \begin{bmatrix} \psi_{i,l} \\ \psi_{i,l} \lambda_{i,l} \end{bmatrix} = 0 \, . \tag{25}$$

The theoretical necessary number of mode shapes is doubled, hence $\Psi_i = [\psi_{i,1} \quad \psi_{i,2} \quad \ldots]$, $\Psi_i \in \mathbb{C}^{N_{dof} \times 2N_{dof}}$. This leads to *complex conjugated* eigenvalues, for i denoted by $\Lambda_i = \mathrm{diag}(\lambda_{i,1},\, \lambda_{i,1},\, \ldots)$ with $\lambda_{l,l+1} = -\zeta_l \omega_l \pm j \omega_l (1 - \zeta_l^2)^{0.5}$. Again a factor β may be used, which allows to determine scaled mode shapes $\bar{\psi}_l = \psi_l \beta_l$. In contrary to the mass-scaling approach, complex mode shapes can be scaled to $-45°$. Then, mechanical parameters are estimated by analysing the sum of outer products (e.g. based on SSI):

$$\hat{M}_i = \left[\sum_{l=1}^{n} \bar{\psi}_{i,l} \lambda_{i,l} \bar{\psi}_{i,l}^T \right]^{-1} , \quad \hat{K} = \left[- \sum_{l=1}^{n} \frac{\bar{\psi}_{i,l} \bar{\psi}_{i,l}^T}{\lambda_{i,l}} \right]^{-1} , \quad \hat{D} = - \sum_{l=1}^{n} \hat{M} \bar{\psi}_{i,l} \lambda_{i,l}^2 \bar{\psi}_{i,l}^T \hat{M} \, . \tag{26}$$

Several methods have been developed to scale mode shapes based on the mass perturbation technique [29–34]. To estimate mechanical parameters, an important rank problem must be considered: If $\hat{F}$ is full-rank with $n \geq p$, the inverse $\hat{F}\hat{K} = I_p$ exists. Very importantly, the rank deficient case $\hat{K} = \hat{F}^{\dagger}$ with $n < p$ leads to $\hat{F}\hat{F}^{\dagger} \neq I_p$.

4 Experimental results of a real structure

4.1 The experimental study

This section covers experimental results of mechanical parameter estimation of the laboratory structure (see figure 1b). The proof of damage localization by SP2E has been given before (see [10]). In this contribution the authors discussed several methods to estimate corresponding mechanical parameters (table 1), which will be applied below. All three methods are based on output-only measurements and mass perturbations (repetition of measurement with known additional mass Δ_M).

Abbreviation	Approach	Equation
<Kronecker>	Kronecker product based method applying state projections.	(22)
<Mode I>	Modal approach based on real eigenvectors.	(24)
<Mode II>	Modal approach employing complex eigenvectors.	(26)

Table 1: Discussed methods to estimate corresponding mechanical parameters

The experimental structure. To apply techniques described above, a cantilever arm (length $6.15\,\mathrm{m}$) in a laboratory at Leipzig University of Applied Sciences was analysed. The modular structure consists of six beam elements with $1\,\mathrm{m}$ length each (cross section IPE200, DIN EN 10 034) and were connected by bolted steel plates. Therefore, stiffness and mass alterations can be applied using additional steel plates. Using a wind excitation by wind machines (random, stationary ambient excitation), structural acceleration responses were measured in lateral direction by twelve uniaxial, piezoelectric accelerometers (equally spaced $100\,\mathrm{cm}$, measurement position $\mathrm{M}_1 \ldots \mathrm{M}_6$, see figure 3).

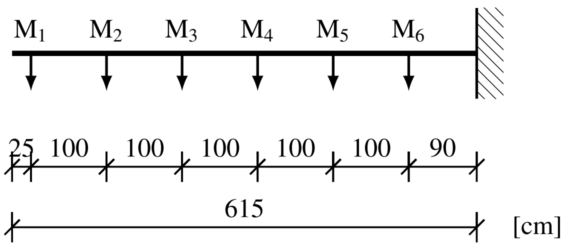

Figure 3: Mechanical system: Cantilever arm

Data processing Measured accelerations had a duration of $30\,\mathrm{min}$ ($f_s = 2\,\mathrm{kHz}$) and were analysed by Welch's method first. For a sufficient statistical population we applied approximately 215 averages by Hanning window ($L = 2^{15}$). The estimated spectrum was used to identify the output-only system: An inverse Fourier transform of spectrum S_y led to covariance matrix function R_y, which was applied in the stochastic subspace identification method. SSI results A and C eventually identified noise poles, which had been suppressed by model reduction techniques afterwards. This led to the identification of six natural frequencies (bending modes in lateral direction).

4.2 Results: Corresponding mechanical parameter estimates

4.2.1 Corresponding mass estimate

In this study all discussed methods led to a mass estimate $\hat{M}$ with a dominant main diagonal, which corresponds to the laboratory structure. Because, corresponding mass estimates are elaborate to analyze (e.g. interpretation of off-diagonal elements), the trace of $\hat{M}$ is used below.

Simulated mass [kg]

17	0	0	0	0	0
0	32	0	0	0	0
0	0	32	0	0	0
0	0	0	32	0	0
0	0	0	0	32	0
0	0	0	0	0	30
1	2	3	4	5	6

<Kronecker> Estimated mass [kg]

1	12.6	1.2	0.4	0.9	-1.4	-4.3
2	3.9	29.8	-4	-1.6	-1.6	-7.9
3	-2.4	1.7	30.9	0.4	0.4	-3.3
4	0.6	2.9	5.4	32.3	1.2	-3.2
5	-0.5	2.4	-3	0.5	32.4	0.7
6	1.2	0.6	-4.8	0.8	0.7	30.5
	1	2	3	4	5	6

<Mode I> Estimated mass [kg]

13.3	3.9	-2.6	0.7	-1.1	0.6
3.9	31.2	-0.1	-0.1	-0.6	-0.2
-2.6	-0.1	31.3	0.9	0.1	0
0.7	-0.1	0.9	31.2	1.2	0.1
-1.1	-0.6	0.1	1.2	30.6	1.3
0.6	-0.2	0	0.1	1.3	29

<Mode II> Estimated mass [kg]

1	13.3	3.9	-2.6	0.7	-1.1	0.6
2	3.9	31.2	-0.1	-0.1	-0.6	-0.3
3	-2.6	-0.1	31.4	1	0.1	-0
4	0.7	-0.1	1	31.2	1.2	0.1
5	-1.1	-0.6	0.1	1.2	30.7	1.3
6	0.6	-0.3	-0	0.1	1.3	29

Figure 4: Estimated corresponding mass $\hat{M}$, for abbreviations see table 1

The results of corresponding mass estimates is given in figure 4. The Kronecker product based method leads to trace$(\hat{M}) = 168.7\,\mathrm{kg}$. Besides that, both modal approaches lead by definition to symmetric parameter matrices with a similar trace of $\hat{M}$, trace$(\hat{M}) = 166.8\,\mathrm{kg}$. The experiments have been repeated two times and structural mass of the laboratory set-up has been repeatedly estimated.

4.2.2 Corresponding stiffness estimate

Stiffness $\bar{K}$ is a central parameter to describe mechanical systems (e.g. relation between external static forces and measured displacements). Corresponding stiffness estimates are given in figure 5. Although all three methods lead to a similar result in comparison to the simulated, analytical stiffness parameters, differences between simulation and real laboratory structure must be emphasized. Possible explanations may be: a) The real stiffness of laboratory clamping end is not infinite, which was presupposed in the Euler-Bernoulli beam simulation, and b) the used Euler-Bernoulli beam equation assumes a constant flexural rigidity EI, which is not exact considering the bolted steel plate connections (figure 1b).

Essentially, the corresponding mass and stiffness estimates can be evaluated similarly. In the results of all methods one may recognize a band parameter matrix. However, the Kronecker

Simulated stiffness [MN/m]

1	2	3	4	5	6
0.5	-1.1	0.8	-0.2	0.1	-0
-1.1	2.9	-2.8	1.2	-0.3	0.1
0.8	-2.8	4.2	-3.2	1.3	-0.4
-0.2	1.2	-3.2	4.3	-3.2	1.5
0.1	-0.3	1.3	-3.2	4.4	-3.8
-0	0.1	-0.4	1.5	-3.8	6.7

<Kronecker> Estimated stiffness [MN/m]

	1	2	3	4	5	6
1	0.6	-1.6	1.6	-1	1	-1.1
2	-1.1	3	-3	1.1	0.5	-1.4
3	0.7	-2.8	4.3	-3.7	2.2	-1.4
4	-0.3	1.3	-3.2	4.3	-3.1	1.1
5	-0	-0.1	1.2	-3.6	5.1	-4.4
6	-0.2	0.8	-1.7	2.9	-4.8	6.8

<Mode I> Estimated stiffness [MN/m]

0.5	-1	0.8	-0.3	0.1	-0
-1	2.9	-2.9	1.5	-0.6	0.2
0.8	-2.9	4.4	-3.5	1.7	-0.7
-0.3	1.5	-3.5	4.8	-3.7	2
0.1	-0.6	1.7	-3.7	4.9	-4.1
-0	0.2	-0.7	2	-4.1	6.2

<Mode II> Estimated stiffness [MN/m]

1	0.5	-1	0.8	-0.3	0.1	-0
2	-1	2.9	-2.9	1.5	-0.5	0.2
3	0.8	-2.9	4.4	-3.5	1.7	-0.7
4	-0.3	1.5	-3.5	4.8	-3.7	2
5	0.1	-0.5	1.7	-3.7	4.9	-4.1
6	-0	0.2	-0.7	2	-4.1	6.2

Figure 5: Estimated corresponding stiffness $\hat{K}$, for abbreviations see table 1

product based method leads to a non-symmetric parameter matrix. In summary, the estimation of corresponding stiffness has been estimated successfully.

5 Conclusions

In this contribution the current progress on the development of damage localization and scaling output-only systems from a general operator notation is shown. At first damage localization based on the *state projection estimation error* (SP2E) method is briefly presented. Modifying this theory, system scaling and mechanical parameter estimation is discussed afterwards. Based on output-only measurements and a mass perturbation technique, this allows to define a mechanical parameter estimation method, which is afterwards compared to two well-known modal approaches using real and complex eigenvectors. Finally, experimental results are shown and analysed. Identifying a real mechanical system, the applicability of the novel *state projections for system scaling* (SP2S) method is confirmed. More results can be found in [9–11, 26]. Some theoretical and practical issues are still open, which should be analysed in the future. These studies may focus on an application at large-scale structures taking varying environmental and operational conditions into account.

Acknowledgements

This research has been financed by the German Research Foundation (grant number 350257805) and Leipzig University of Applied Sciences (grant number K-7531.20/544-9). The authors acknowledge gratefully the granted support.

References

[1] A. Cunha, E. Caetano, F. Magalhães, and C. Moutinho. Recent perspectives in dynamic testing and monitoring of bridges. *Structural Control and Health Monitoring*, 20(6):853–877, 2013.

[2] P.L. Faurre. Stochastic realization algorithms. *System Identification: Advances and Case Studies*, 126:1–25, 1976.

[3] P. Van Overschee and B. De Moor. *Subspace Identification for Linear Systems: Theory, Implementation, Applications*. Kluwer Academic Publishers, 1996.

[4] T. Katayama. Realization of stochastic systems with exogenous inputs and subspace identification methods. *Automatica*, 35(10):1635–1652, 1999.

[5] B. Peeters and G. De Roeck. Reference-based stochastic subspace identification for output-only modal analysis. *Mechanical Systems and Signal Processing*, 13(6):855–878, 1999.

[6] F. Ubertini, C. Gentile, and A.L. Materazzi. Automated modal identification in operational conditions and its application to bridges. *Engineering Structures*, 46:264–278, 2013.

[7] E. Reynders, K. Maes, G. Lombaert, and G. De Roeck. Uncertainty quantification in operational modal analysis with stochastic subspace identification: validation and applications. *Mechanical Systems and Signal Processing*, 66:13–30, 2016.

[8] A. Lenzen and M. Vollmering. A new technique for damage localisation using estimates in Krein spaces. *Proceedings of the 6th International Operational Modal Analysis Conference*, 2015.

[9] A. Lenzen and M. Vollmering. An output-only damage identification method based on $\mathcal{H}_\infty$ theory and state projection estimation error (SP2E). *Structural Control and Health Monitoring*, 2017.

[10] A. Lenzen and M. Vollmering. On experimental damage localization by SP2E: Application of $\mathcal{H}^\infty$ estimation and oblique projections. *Mechanical Systems and Signal Processing*, 104:648–662, 2018.

[11] M. Vollmering and A. Lenzen. Theory and numerical application of damage localization method state projection estimation error (SP2E). *Structural Control and Health Monitoring*, 25(10):e2237, 2018.

[12] S. Wernitz, D. Pache, T. Grießmann, and R. Rolfes. Damage localization with SP2E under changing conditions. *The 12th International Workshop on Structural Health Monitoring*, 2019.

[13] D. Simon. *Optimal State Estimation: Kalman, H_∞, and Nonlinear Approaches*. Wiley, 2006.

[14] B. Hassibi, A.H. Sayed, and T. Kailath. *Indefinite-Quadratic Estimation and Control: A Unified Approach to H^2 and H^∞ Theories*. SIAM Studies in Applied Mathematics. Society for Industrial and Applied Mathematics, 1999.

[15] R.N. Banavar. *A game theoretic approach to linear dynamic estimation*. PhD thesis, Texas University, Austin, 1992.

[16] K. Takaba and T. Katayama. Discrete-time H_∞ algebraic riccati equation and parametrization of all H_∞ filters. *International Journal of Control*, 64(6):1129–1149, 1996.

[17] R.S. Mangoubi. *Robust Estimation and Failure Detection: A Concise Treatment*. Advances in Industrial Control. Springer London, 2012.

[18] K. Zhou, J.C. Doyle, and K. Glover. *Robust and Optimal Control*. Feher/Prentice Hall Digital and. Prentice Hall, 1996.

[19] P. Gahinet and P. Apkarian. A linear matrix inequality approach to $\mathcal{H}_\infty$ control. *International journal of robust and nonlinear control*, 4(4):421–448, 1994.

[20] T. Iwasaki and R.E. Skelton. All controllers for the general $\mathcal{H}_\infty$ control problem: LMI existence conditions and state space formulas. *Automatica*, 30(8):1307–1317, 1994.

[21] C. Scherer, P. Gahinet, and M. Chilali. Multiobjective output-feedback control via LMI optimization. *IEEE Transactions on automatic control*, 42(7):896–911, 1997.

[22] H. Gao and X. Li. *Robust Filtering for Uncertain Systems: A Parameter-Dependent Approach*. Communications and Control Engineering. Springer International Publishing, 2014.

[23] A.H. Sayed, B. Hassibi, and T. Kailath. Inertia conditions for the minimization of quadratic forms in indefinite metric spaces. *Recent Developments in Operator Theory and Its Applications*, pages 309–347, 1996.

[24] V. Sima. *Algorithms for Linear-Quadratic Optimization*. Chapman & Hall/CRC Pure and Applied Mathematics. Taylor & Francis, 1996.

[25] V. Ionescu, C. Oară, and M. Weiss. *Generalized Riccati Theory and Robust Control: A Popov Function Approach*. Wiley, 1999.

[26] A. Lenzen and M. Vollmering. Mechanical system scaling based on output only identification and mass perturbations by state projections. *Mechanical Systems and Signal Processing*, Special Issue in Honor of Professor Lothar Gaul:106863, 2020.

[27] C. Ebert. *Systemidentifikation zur Modellierung mechanischer Strukturen: Markovparameter zur experimentellen Schadenserfassung*. Dissertation, Universität Siegen, 2013.

[28] E. Balmès. New results on the identification of normal modes from experimental complex modes. *Mechanical Systems and Signal Processing*, 11(2):229–243, 1997.

[29] E. Parloo, P. Verboven, G. Guillaume, and M. van Overmeire. Sensitivity-based operational mode shape normalisation. *Mechanical Systems and Signal Processing*, 16(5):757–767, 2002.

[30] R. Brincker and P. Andersen. A way of getting scaled mode shapes in output only modal testing. In *Proc. 21st Int. Modal Analysis Conference, Kissimmee, FL*, 2003.

[31] D. Bernal. Modal scaling from known mass perturbations. *Journal of engineering mechanics*, 130(9):1083–1088, 2004.

[32] D. Bernal. A receptance based formulation for modal scaling using mass perturbations. *Mechanical systems and Signal processing*, 25(2):621–629, 2011.

[33] M.M. Khatibi, M.R. Ashory, A. Malekjafarian, and R. Brincker. Mass–stiffness change method for scaling of operational mode shapes. *Mechanical Systems and Signal Processing*, 26:34–59, 2012.

[34] D. Bernal. Complex eigenvector scaling from mass perturbations. *Mechanical Systems and Signal Processing*, 45(1):80–90, 2014.